Terra Nova

doi: 10.1111/ter.12216

Reloca Slide: an ~24 km^3 submarine mass-wasting event in response to over-steepening and failure of the central Chilean continental slope

Eduardo Contreras-Reyes,[1] David Völker,[2] Jörg Bialas,[3] Eduardo Moscoso[4] and Ingo Grevemeyer[3]

[1]*Departamento de Geofísica, Facultad de Ciencias Físicas y Matemáticas, Universidad de Chile, Santiago, Chile;* [2]*MARUM, Zentrum für Marine Umweltwissenschaften der Universität Bremen, Bremen, Germany;* [3]*GEOMAR Helmholtz Zentrum für Ozeanforschung, Kiel, Germany;* [4]*Pontificia Universidad Católica de Valparaíso, Escuela de Ciencias del Mar,Av. Altamirano 1480, Valparaíso, Chile*

ABSTRACT

Reloca Slide is the relict of an ~24-km^3 submarine slope collapse at the base of the convergent continental margin of central Chile. Bathymetric and seismic data show that directly to the north and south of the slide the lower continental slope is steep (~10°), the deformation front is shifted landwards by 10–15 km, and the frontal accretionary prism is uplifted. In contrast, ~80 km to the north the lower continental margin presents a lower slope angle of about 4° and a wide frontal accretionary prism. We propose that high effective basal friction conditions at the base of the accretionary prism favoured basal accretion of sediment and over-steepening of the continental slope, producing massive submarine mass wasting in the Reloca region. This area also spatially correlates with a zone of low coseismic slip of the 2010 Maule megathrust earthquake, which is consistent with high basal frictional coefficients.

Terra Nova, 28: 257–264, 2016

Introduction

At convergent margins with sediment-filled trenches, accretionary prisms form through the transfer of material from the subducting plate to the overriding plate. Accretionary prisms can grow by frontal offscraping at the trench and/or by basal sediment accretion (underplating) at the base of the accretionary prism. The mechanical state of accretionary prisms can be described in terms of the critical Coulomb wedge model (Davis *et al.,* 1983; Dahlen, 1984; Lallemand *et al.,* 1994). This model considers the geometry of the accretionary prism as a wedge defined by the continental slope α and the basal dip β (Fig. 1). If cohesion is neglected, the submarine accretionary prism can be modelled as a critically tapered wedge, the shape of which is a function of its internal and basal coefficients of friction, μ and μ_b, and its internal and basal fluid pressure ratios (Davis *et al.,* 1983; Dahlen, 1984; Lallemand *et al.,* 1994). The solutions of the critical Coulomb wedge theory correspond to an envelope curve in a graph of α vs. β involving compressional and extensional regimes around a stability zone. Based on this theory, continental margins have been classified globally as accretionary, erosive or non-accretionary margins according to their α and β values (e.g. Lallemand *et al.,* 1994). The feasibility of this simple global classification suggests that the detailed analysis of the slope and basal angles is a key tool in the study of the stress condition of the continental wedge and its long-term deformation (see supplementary material for further details of the formulations and assumptions of the critical Coulomb wedge theory). In particular, the critical Coulomb wedge theory predicts that high values of α should be associated with high basal friction values (Davis *et al.,* 1983; Dahlen, 1984; Lallemand *et al.,* 1994). Hence, along-strike changes in the slope angle can be indicative of spatial variability in the long-term basal friction.

The central Chile (34°–36°S) convergent margin presents a pronounced diversity in its continental slope morphology and the size of the accretionary prism (e.g. Contreras-Reyes *et al.,* 2013), as well as in the basal friction properties at the interplate contact (e.g. Cubas *et al.,* 2013; Maksymowicz, 2015; Maksymowicz *et al.,* 2015). The trench presents a flat floor due to the massive infill of turbidity-derived beds, only disrupted by an approximately N–S trending trench axial channel located 5–30 km seawards of the deformation front. This flat trench floor morphology changes abruptly at ~35.6°S, where deposits of the Reloca Slide, a massive mass-wasting event, cover the trench floor (Figs 2 and 3). The volume of the mass-wasting deposit has been estimated at ~24 km^3 (Völker *et al.,* 2009). The lower continental slope facing the blocky deposits of the Reloca Slide is characterized by a very steep and high headscarp that forms a spoon-shaped indentation. Adjacent to the headscarp, both to the north and south, the apparently unfailed lower continental slope is steep, with α values of ~10° (Fig. 2). Further to the north (≥80 km north of the Reloca Slide), the continental slope is smooth ($\alpha = \sim 4°$; Fig. 2). Hereafter, we refer to the region of the Chilean margin between 34°S and 35.3°S as the Mataquito Segment, and to the region around the Reloca Slide (between 35.3°S and 35.7°S; Fig. 2) as the Reloca Segment.

Mechanisms explaining the diversity in the continental slope morphology along the central Chilean margin are poorly understood and can be

Correspondence: Professor Eduardo Contreras-Reyes, Departamento de Geofísica, Universidad de Chile, Blanco Encalada 2002, Santiago 8370449, Chile. Tel.: +0056 2 29784296; e-mails: econtreras@dgf.uchile.cl; edcontrr@gmail.com

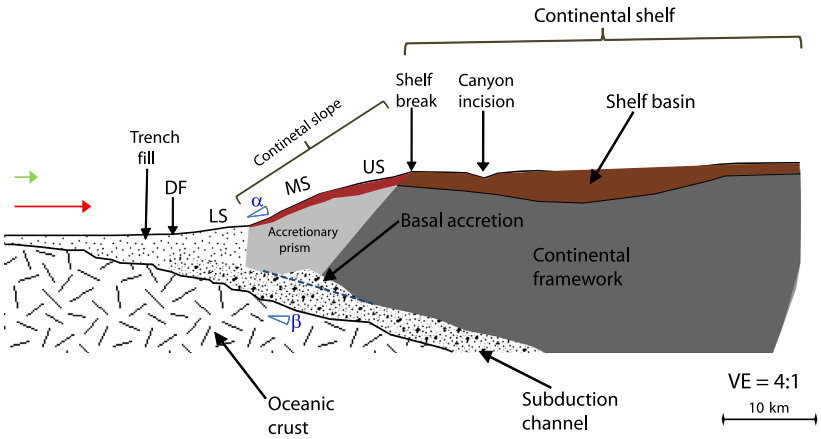

Fig. 1 Typical scheme of the south central Chilean convergent margin, with the continental slope and basal angles α and β respectively. DF, deformation front; LS, lower slope; MS, middle slope; US, upper slope. Red and green arrows represent the distance displaced by the slab in 100 ka, and 18 ka, respectively. The landward end of the accretionary prism has been defined by seismic refraction data as an abrupt horizontal velocity gradient, which is interpreted as the location of the contact between the accretionary prism and the continental framework (Contreras-Reyes *et al.,* 2013). This contact is usually found below the shelf break or the transition from the upper continental slope to the continental shelf along the central Chilean margin. The high average sedimentation rate since the Pliocene due to fast denudation of the Andes and the steady decrease of the Nazca–South America convergence rate shifted the margin from erosive to accretionary during the Pliocene (Kukowski and Oncken, 2006; Melnick and Echtler, 2006; Somoza, 1998). This process facilitated the formation of accretionary prisms 50–150 km^2 (Contreras-Reyes *et al.,* 2013). These sizes for the accretionary prisms are not consistent with a long history of accretion with the current deformation style (Bangs and Cande, 1997; Contreras-Reyes *et al.,* 2013), and an important amount of subducted and underplated sediment is likely in the south central Chilean margin.

related to basal properties of the underthrust interface and the style of sediment accretion (dominance of frontal vs. basal accretion). In order to examine the causes of the morphological diversity, we use seismic and bathymetric constraints along two seismic profiles oriented roughly perpendicular to the trench axis (Fig. 2). The study of lower continental slope failure is important to understand the potential tsunamigenic effect in this highly active convergent margin, where the last destructive megathrust earthquake occurred on February 27, 2010 (Mw 8.8).

Morphotectonic structures of the central Chile margin (34°–36°S)

The central Chile convergent margin (34°–36°S) is characterized by the subduction of the oceanic Nazca plate beneath the continental South American plate at a convergence rate of 6.6 cm a^{-1} with a convergence azimuth of N78°E (Angermann *et al.,* 1999). The trench fill in this region is 1–2 km thick (Völker *et al.,* 2013), and sediment supply to the trench is mainly controlled by enhanced erosion during glaciation periods, denudation of the Andean Cordillera and sediment transport via submarine canyons (Thornburg *et al.,* 1990; Völker *et al.*, 2006). The frontalmost part of the margin consists of an accretionary prism 30–50 km wide (Moscoso *et al.,* 2011; Contreras-Reyes *et al.,* 2013). The continental slope from the shelf break to the trench is subdivided into (i) a broad, gently seaward-dipping upper slope, (ii) a middle slope with asymmetric slope basins (González, 1989; Geersen *et al.,* 2011; Fig. 2A) and (iii) the present accretionary prism, which forms the lowermost part of the slope and characteristically has the highest gradient. This steep lowermost slope ends at the flat, sediment-filled trench (Völker *et al.,* 2013).

The most remarkable morphologic feature at the base of the continental slope in our study area is the Reloca Slide. It is exceptionally evident as a mass-wasting event because of the proximity of the evacuation area and the displaced material and because of the good preservation and textbook morphology of both. The evacuation area at the lower slope takes the form of a spoon-shaped indentation into the lowermost slope with a headscarp that is clearly defined by a sudden gradient change of the lower continental slope (Fig. 3). The timing of the event is not well constrained but it postdates the incision of the so-called Trench Axial Channel, as the seawardmost extension of the debris fan buried a part of that channel. Some (fore-runner) blocks of the slide mass crossed the channel, riding on top of the debris (Fig 3, detail map). As the Trench Axial Channel appears to have been actively excavated during glacial sea-level lowstands (Thornburg *et al.*, 1990), this implies a post-Last Glacial Maximum (LGM) age of <18 ka. The Reloca Slide is not the only mass-wasting event along the Chilean margin. For instance, Geersen *et al.* (2011) reported three Pleistocene giant slope failures in the Arauco area off Chile (36.5°–39°S) with estimated volumes between 253 and 472 km^3. These authors used seismic reflection constraints to estimate ages between 250 and 560 ka for these three slides (see Supplementary material for further details). Apart from these much older giant slides, however, the size of the Reloca Slide is exceptional.

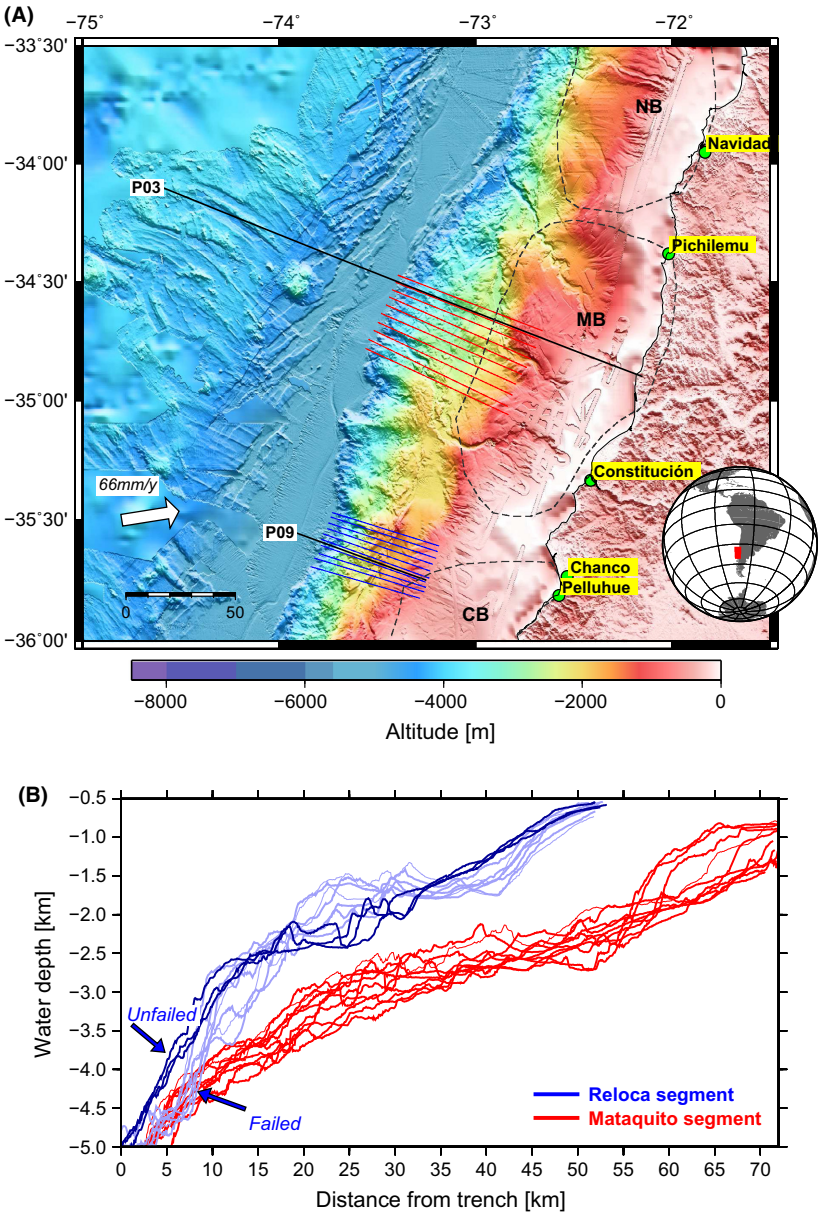

Fig. 2 (A) Bathymetric map of the Maule District of Central Chile based on swath bathymetry data from the expeditions of RV SONNE, RV METEOR and RRS JAMES COOK. Black lines denote the wide-angle seismic profiles studied by Moscoso *et al.* (2011), P03, and this work, P09. Red and blue lines indicate the bathymetric profiles extracted from the Mataquito and Reloca Segments, respectively, that are shown in (B). The continental shelf is characterized by forearc or shelf basins (NB, Navidad Basin; MB, Mataquito Basin; and CB, Chanco Basin). (B) Bathymetric profiles along the continental slope extracted from the Mataquito (red) and Reloca (dark and light blue) Segments. The Reloca Segment presents a steep to extremely steep lower continental slope. Profiles that run across the headscarp of the Reloca Slide are in light blue (failed slope); profiles across the unfailed slope in the Reloca Segment are in dark blue. In contrast, the Mataquito Segment presents a gentle continental slope with a low α value of ~4°.

Seismic results

We present 2-D velocity–depth models along two wide-angle seismic profiles (locations in Fig. 2). Figure 4 presents the 2-D seismic velocity models for both profiles, showing the sediment-flooded trench, the accretionary prism, the top of the subducting oceanic crust and the continental slope and its sediment cover. Both velocity–depth models terminate a few km seaward of the shelf break. Profile P09 crosses the Reloca Slide. The seismic experiment, seismic modelling, seismic record data examples and data fit are presented in the Supplementary Material.

Along seismic line P09, the bathymetric profile presents a very steep lower continental slope ($\alpha = \sim 22°$) highlighted by the Reloca mass-wasting products at its base. The slope sediment cover along this line is up to 3.6 km thick and overlies an accretionary prism with seismic velocities ranging between 2.5 and 4.5 km s^{-1}. The deformation front is shifted landwards by 10–15 km in relation to the Mataquito Segment. Along seismic profile P03, in contrast, the trench contains less sediment, and the continental slope is smooth with a steady continental slope angle of ~4.2°. The accretionary prism is relatively wide (40–50 km), and its landward edge is defined by an abrupt horizontal velocity gradient located a few km seawards of the shelf break (Moscoso *et al.*, 2011).

Discussion and conclusions

The Reloca Segment is characterized by a remarkably steep and uplifted lower continental slope, and we propose that it had reached an overcritical angle that led to a large mass-wasting event. The uplifted region overlies a region with similar seismic velocities, which suggests basal accretion of sediment rather than seamount subduction as the cause of the uplifted lower continental slope. Usually, basaltic seamounts present higher seismic velocities than sedimentary rocks on the flanks of the seamount (e.g. Kaneda *et al.*, 2010), which is not observed along seismic line P09 (Fig. 4). Thus, a potential cause for the Reloca Slide is oversteepening of the lower slope caused by basal accretion of subducted sediments, accompanied by high uplift rates. In this sense, the Reloca Segment was characterized by higher uplift rates compared to the smoother continental slope southwards and northwards.

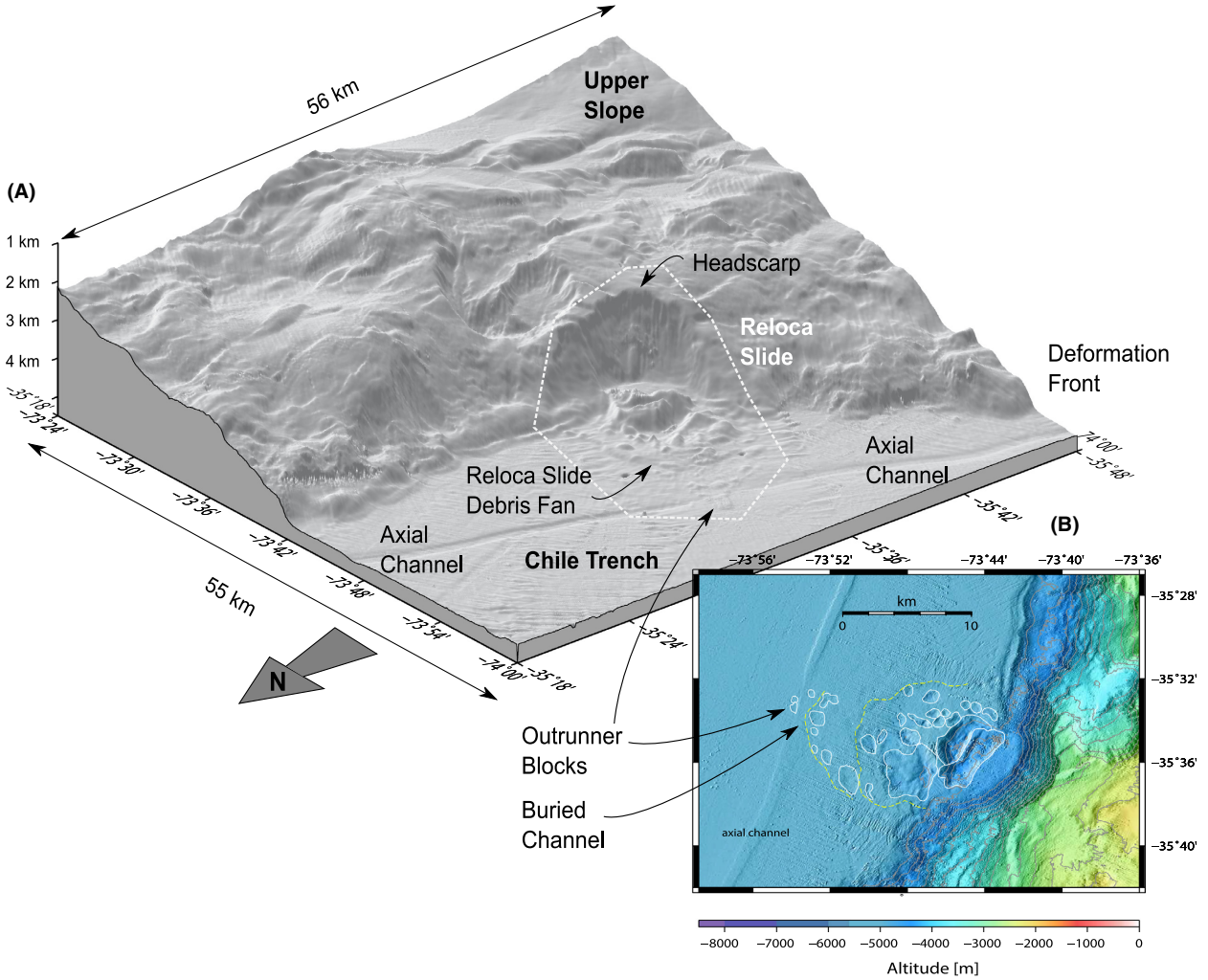

Fig. 3 (A) Detailed 3-D view of the Reloca Slide morphology looking from NW (azimuth 300°). The perspective view shows the flat plain of the sediment-flooded Chile Trench, the axial channel within the trench and both the evacuation area (headscarp and spoon-shaped depression) and the products of the sliding event (blocky deposits resting on a cone of debris). It can also be seen that the sliding event postdates the incision of the axial channel, as the toe of the slide debris buries a part of the channel. Within the evacuation area, the gliding plane is exposed as a 2000 m high and up to 40° steep, slightly curved surface that ends at the trench. (B) In the trench and directly facing this gliding plane, the slide deposits are preserved as clusters of individual blocks, embedded within a 60 m high fan of debris that stretches more than half way across the flat floor of the Chile Trench. About 66% of the estimated total volume of the slide is contained in only three blocks that rise up to 700 m from the trench floor, while about 25 blocks of smaller volume are detectable and, together with the debris fan, make up the rest of the volume (Völker *et al.,* 2009).

Over-steepening of continental slopes is a common feature where basal accretion or sediment subduction takes place (e.g. Contardo *et al.,* 2008). Furthermore, basal accretion is favoured at accretionary margins where accelerated sediment supply to the trench, and thus higher load, causes local subsidence/down-deflection of the oceanic plate near the trench (e.g. Contreras-Reyes *et al.,* 2013). This process leads to subduction of larger sediment volumes to the base of the accretionary prism, which in turn drives basal underplating and pronounced uplift (e.g. Lohrmann *et al.*, 2001; Contardo *et al.,* 2008). The sediment volume input at the trench is larger in the Reloca Segment (~140 km² Ma^{-1} trench km^{-1}) than in the Mataquito Segment (~70 km^2 Ma^{-1} trench km^{-1}). Consistently, the bathymetric data show that the trench basin is much wider in the Reloca Segment (Fig. 2). The higher sediment supply to the trench in the Reloca Segment could be a consequence of material sourced from the massive Bío-Bío Fan and transported northwards within the trench (Völker *et al.*, 2006) and/or sediment provided from the continent during interglacial periods (e.g. Blumberg *et al.,* 2008). We speculate that sediment transport down the continental slope is more effective in the Reloca Segment because of its location at the edge of the Chanco Shelf Basin. In contrast, less

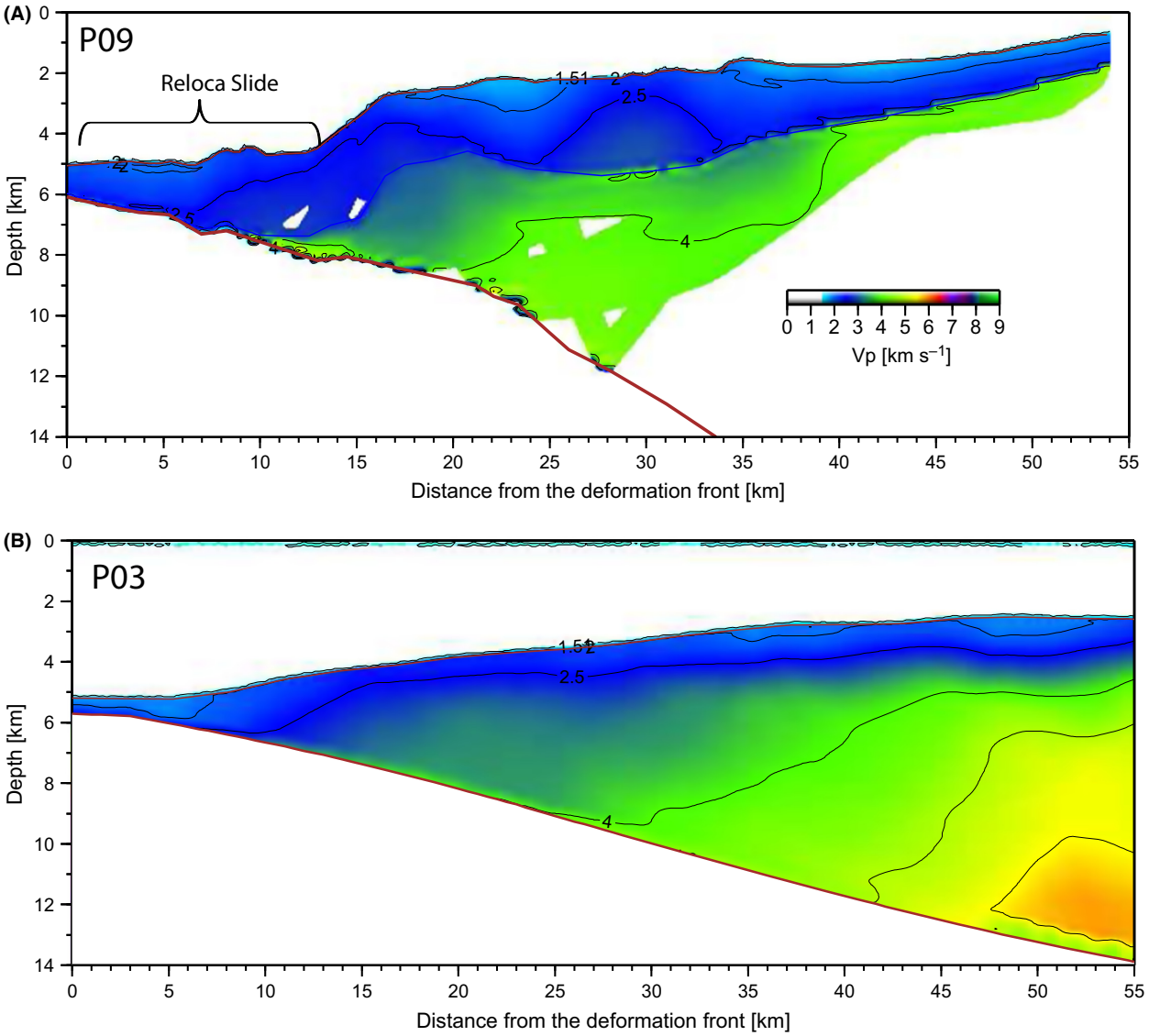

Fig. 4 Comparison of the 2-D velocity–depth models between profiles (A) P09 (this work) and (B) P03 (Moscoso *et al.*, 2011). Please note that the velocity–depth models shown are located seawards of the shelf break and landward of the trench axial channel (see Fig. 1 for a schematic cartoon). Unconsolidated sediments with typical velocities of 1.7–2.5 km a^{-1} define the sedimentary slope cover and the most seaward part of the accretionary prism as well as the trench fill.

sediment reaches the trench in the Mataquito Segment due to the presence of the large Maule shelf basin (González, 1989) which likely acts as a trap for large volumes of transported sediment before it reaches the trench in interglacial periods (see Fig. 2 for location of the forearc basins). Thus, the larger sediment volume at the trench in the Reloca segment might favour basal accretion of sediment.

Basal accretion is also favoured by high basal friction conditions at the plate interface, while low basal friction favours frontal accretion of a wedge with low taper angle and slow uplift rates (e.g. Kukowski *et al.*, 2002; Contardo *et al.*, 2008). Thus, slope over-steepening in the Reloca Segment is likely caused by basal sediment accretion controlled by the high basal friction conditions in combination with a local maximum in sediment supply. Evidence for high basal friction properties in the Reloca Segment comes from basal estimates obtained by Coulomb wedge modelling based on bathymetric and gravimetric data that derives the long-term interplate friction coefficient off central Chile (34°–36°S) (Maksymowicz, 2015; Maksymowicz *et al.*, 2015). These authors estimated high effective basal friction coefficients for the continental slope landwards of the Reloca Slide (μ_b = 0.47 for the lower slope and μ_b = 0.4 for the middle slope). These values are noticeably higher than those estimated further north (μ_b = 0.36 for the lower slope and μ_b = 0.38 for the middle slope) and in fact are the highest along central Chile (Maksymowicz, 2015).

The Mataquito and Reloca Segments form part of the rupture area of the Mw = 8.8 Maule megathrust earthquake (MEQ) that occurred on 27 February 2010 (e.g. Moreno *et al.,* 2012; Maksymowicz *et al.,* 2015). Most of the coseismic slip models indicate that the Mataquito Segment spatially correlates with the highest slip patch (~16 m) of the MEQ (e.g. Delouis *et al.*, 2010; Lorito *et al.,* 2011; Moreno *et al.,* 2012). A secondary slip maximum of 8–10 m appears south of the epicentre. Due to differences in the geodetic databases and in the inversion algorithms used by different authors, details of the slip models for the Maule earthquake differ over the models, but their main features are similar (see supplementary material). For our interpretation, we use the coseismic slip model of Moreno *et al.* (2012), which combines GPS and InSAR observations and includes realistic slab geometry (Fig. 5).

The Reloca Segment correlates spatially with an area of minimum coseismic slip (Fig. 5), which is consistent with high μ_b values of 0.47 for the trenchward part of the interplate contact (Maksymowicz *et al.*, 2015). Similarly, Cubas *et al.* (2013), based on bathymetry and Coloumb wedge theory analysis, also concluded low basal friction coefficients for the highest slip patch of the Maule earthquake. Fagereng (2011) and Cubas *et al.* (2013) report similar findings for the Hikurangi subduction zone (New Zealand) and the Japanese subduction zone, respectively. This observation suggests that regions with steep continental slopes at high basal friction conditions might experience little slip during the coseismic period of megathrust earthquakes. Geersen *et al.* (2011) claimed that the northern termination of the rupture area of the great 1960 Valdivia earthquake Mw = 9.5 (at Arauco Peninsula) coincides with a trench segment that is filled with the debris of a Pleistocene giant slope failure. As that material has been entering the subduction zone ever since, Geersen *et al.* (2013) speculate that the halting of the northward propagation of earthquake slip at this particular place was due to changes in the mechanical behaviour of the plate interface induced by the subducting slope failure debris.

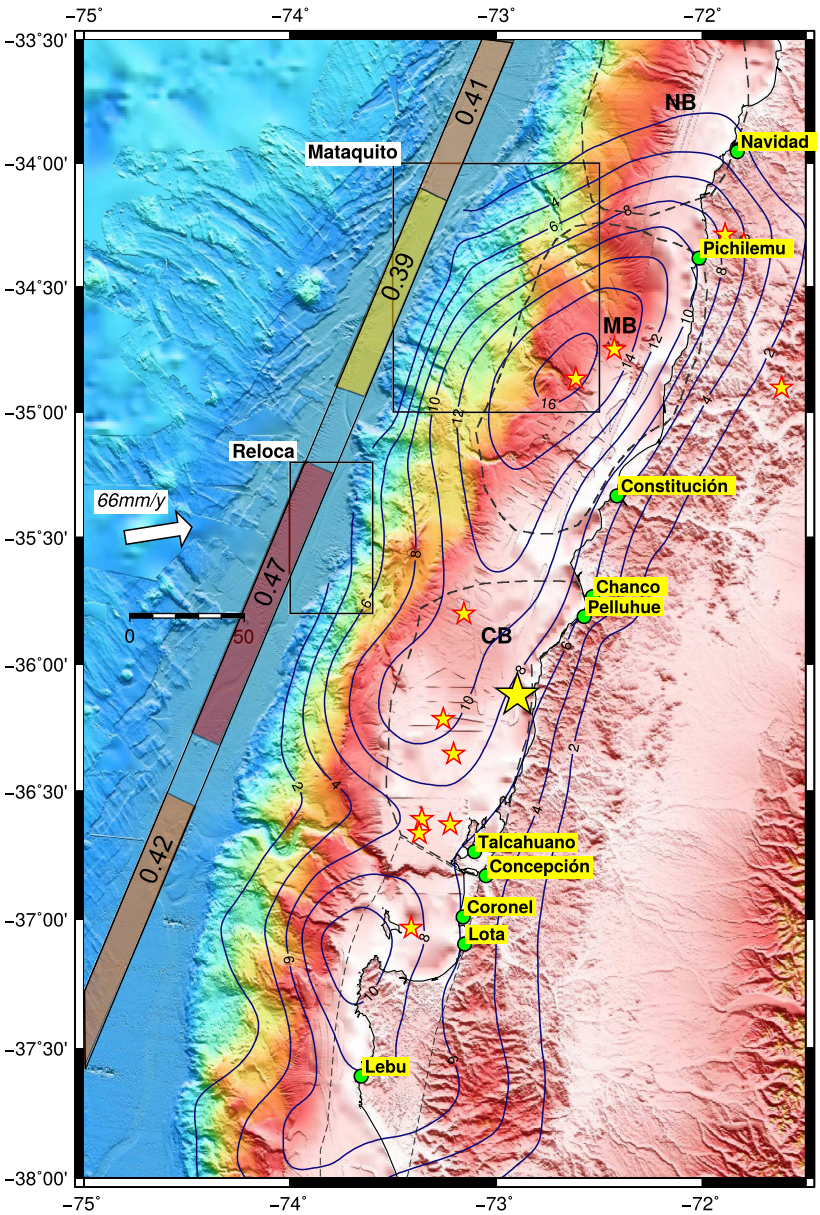

Fig. 5 Rupture area of the Maule Mw 8.8 earthquake, and high resolution bathymetric data. The big yellow star shows the epicentre of the Maule earthquake determined by the *Centro Sismológico Nacional of the Universidad de Chile*. The blue curves are iso-contours of slip during the Maule earthquake taken from the coseismic slip model of Moreno *et al.* (2012). The basal friction coefficient values shown are based on the Coloumb wedge models of Maksymowicz *et al.* (2015) for the seawardmost part of the interplate contact (beneath the lower slope).

We infer that the reduction in the shear yield stress (or critical shear stress required for failure) due to low basal friction coefficients facilitates the concentration of large coseismic slip during an earthquake. However, the frictional variations along the interplate contact are a complex interplay between heterogeneities of the accumulated stresses and irregular rheological conditions at the seismogenic contact. Moreover, interpretations are extremely sensitive to the accuracy of the geodetic coseismic slip models, the uncertainties of which are particularly high offshore (Moreno *et al.,* 2012). Thus, marine geodetic data of high resolution are

necessary to understand the interplay between massive mass-wasting events and rupture of megathrust earthquakes.

Acknowledgements

This work was supported by the Chilean National Science Foundation FONDECYT grant 1130004. Sonderforschungsbereich 574 (Special Research Area) 'Volatiles and Fluids in Subduction Zones', funded by the German Research Foundation, enabled acquisition of seismic data and contributed to the bathymetric map. We thank Andrés Folguera, Mark Cloos, Marcos Moreno and the Associate Editor Vincenzo Pascucci for constructive reviews of the manuscript.

References

Angermann, D., Klotz, J. and Reigber, C., 1999. Spacegeodetic estimation of the Nazca South America Euler vector. *Earth Planet. Sci. Lett.*, **171**(3), 329–334.

Bangs, N.L. and Cande, S.C., 1997. Episodic development of a convergent margin inferred from structures and processes along the southern Chile margin. *Tectonics*, **16**(3), 489–503.

Blumberg, S., Lamy, F., Arz, H.W., Echtler, H.P., Wiedicke, M., Haug, G.H. and Oncken, O., 2008. Turbiditic trench deposits at the south-Chilean active margin: a Pleistocene-Holocene record of climatic and tectonics. *Earth Planet. Sci. Lett.*, **268**, 526–539.

Contardo, X., Cembrano, J., Jensen, A. and Díaz-Naveas, J., 2008. Tectono-sedimentary evolution of marine slope basins in the Chilean forearc (33°30′–36°50′S): insights into their link with the subduction process. *Tectonophysics*, **459**(1–4), 206–218.

Contreras-Reyes, E., Jara, J., Maksymowicz, A. and Weinrebe, W., 2013. Sediment loading at the southern Chilean trench and its tectonic implications. *J. Geodyn.*, **66**, 134–145.

Cubas, N., Avouac, J.P., Soulomiac, P. and Leroy, Y., 2013. Megathrust friction determined from mechanical analysis of the forearc in the Maule earthquake area. *Earth Planet. Sci. Lett.*, **381**, 92–103.

Dahlen, F.A., 1984. Noncohesive critical Coulomb wedges: an exact solution. *J. Geophys. Res.*, **89**(10), 125–133.

Davis, D.M., Suppe, J. and Dahlen, F.A., 1983. Mechanics of fold- and thrust belts and accretionary wedges. *J. Geophys. Res.*, **88**, 1153–1172.

Delouis, B., Nocquet, J.-M. and Valle, M., 2010. Slip distribution of the February 27, 2010 Mw = 8.8 Maule Earthquake, central Chile, from static and high-rate GPS, InSAR, and broadband teleseismic data. *Geophys. Res. Lett.*, **37**, L17305.

Fagereng, A., 2011. Wedge geometry, mechanical strength, and interseismic coupling of the Hikurangi subduction thrust, New Zealand. *Tectonophysics*, **507**, 26–30. http://dx.doi.org/10.1016/j.tecto.2011.05.004.

Geersen, J., Völker, D., Behrmann, J.H., Reichert, C. and Krastel, S., 2011. Pleistocene giant slope failures offshore Arauco Peninsula, Southern Chile. *J. Geol. Soc.*, **168**, 1237–1248.

Geersen, J., Völker, D., Behrmann, J.H., Kläschen, D., Weinrebe, W., Krastel, S. and Reichert, C., 2013. Seismic rupture during the 1960 Great Chile and the 2010 Maule earthquakes limited by a giant Pleistocene submarine slope failure. *Terra Nova*, **25**, 472–477.

González, E., 1989. Hydrocarbon resources in the coastal zone of Chile. In: *Geology of the Andes and its relation to hydrocarbon and mineral resources* (G. Ericksen, et al. ed.), Earth Science Series, vol. 11, pp. 383–404. Circum-Pacific Council for Energy and Mineral Resources, Houston, Texas.

Kaneda, K., Kodaira, D., Nishizawa, A., Morishita, T. and Takahashi, N., 2010. Structural evolution of preexisting oceanic crust through intraplate igneous activities in the Marcus-Wake seamount chain. *G-cubed*, **11**, Q10014. doi:10.1029/2010GC003231

Kukowski, N. and Oncken, O., 2006. Subduction erosion: the "normal" mode of forearc material transfer along the Chilean margin?. In: *Frontiers in Earth Sciences, vol. 3, The Andes: Active Subduction Orogeny* (O. Oncken *et al.*, eds), pp. 217–236, Springer, Berlin.

Kukowski, N., Lallemand, S., Malavieille, J., Gustcher, M.-A. and Reston, T., 2002. Mechanical decoupling and basal duplex formation observed in sandbox experiments with application to the western Mediterranean Ridge accretionary complex. *Mar. Geol.*, **186**, 29–42.

Lallemand, S.E., Schnurle, P. and Malavieille, J., 1994. Coulomb theory applied to accretionary and nonaccretionary wedges—possible causes for tectonic erosion and/or frontal accretion. *J. Geophys. Res.*, **99**, 12033–12055.

Lohrmann, I., Kukowski, N., Oncken, O., 2001. Erosive and accretive mass transfer modes and related deformation at the Chilean forearc – results of 2D scaled sandbox experiments. I. Scientific Report for Research Period 1999–2001. Collaborative Research Center SFB 267. Berlin, Potsdam, pp. 395–421.

Lorito, S., Romano, F., Atzori, S., Tong, X., Avallone, A., McCloskey, J., Cocco, M., Boschi, E. and Piatanesi, A., 2011. Limited overlap between the seismic gap and coseismic slip of the great 2010 Chile earthquake. *Nature Geosci.*, **4**, 173–177.

Maksymowicz, A., 2015. The geometry of the Chilean continental wedge: tectonic segmentation of subduction processes off Chile. *Tectonophysics*, **659**, 183–196. doi: dx.doi.org/10.1016/j.tecto.2015.08.007

Maksymowicz, A., Tréhu, A., Conterras-Reyes, E. and Ruiz, S., 2015. Density-depth model of the continental wedge at the maximum slip segment of the Maule Mw8.8 megathrust earthquake. *Earth Planet. Sci. Lett.*, **409**, 265–277.

Melnick, D. and Echtler, H., 2006. Inversion of forearc basins in south-central Chile caused by rapid glacial age trench fill. *Geology*, **34**(9), 709–712.

Moreno, M., Melnick, D., Rosenau, M., Baez, J., Klotz, J., Oncken, O., Tassara, A., Chen, J., Bataille, K., Bevis, M., Socquet, A., Bolte, J., Vigny, C., Brooks, B., Ryder, I., Grund, V., Smalley, B., Carrizo, D., Bartsch, M. and Hase, H., 2012. Toward understanding tectonic control on the Mw 8.8 Maule Chile earthquake. *Earth. Planet. Sci. Lett.*, **321**, 152–165.

Moscoso, E., Grevemeyer, I., Contreras-Reyes, E., Flueh, E.R., Dzierma, Y., Rabbel, W. and Thorwart, M., 2011. Revealing the deep structure and rupture plane of the 2010 Maule, Chile earthquake (Mw = 8.8) using wide angle seismic data. *Earth Planet. Sci. Lett.*, **307**, 147–155.

Somoza, R., 1998. Updated Nazca (Farallon)-South America relative motions during the last 40 My: implications for mountain building in the Central Andean region. *J. South. Am. Earth. Sci*, **11**(3), 211–215.

Thornburg, T.M., Kulm, L.D. and Hussong, D.M., 1990. Submarine fan development in the southern Chile Trench - a dynamic interplay of tectonics and sedimentation. *Geol. Soc. Am. Bull.*, **102**, 1658–1680.

Voelker, D., Wiedicke, M., Ladage, S., Gaedicke, C., Reichert, C., Rauch, K., Kramer, W. and Heubeck, C., 2006. Latitudinal variation in sedimentary processes in the Peru-Chile trench off central Chile. In: *Frontiers in Earth Sciences: The Andes—Active Subduction Orogeny* (O. Oncken, et al., eds.), pp. 193–216. Springer, Berlin.

Völker, D., Weinrebe1, W., Behrmann, J.H., Bialas, J. and Klaeschen, D., 2009. Mass wasting at the base of the south central Chilean continental

margin: the Reloca Slide. *Adv. Geosci.*, **22**, 155–167.
Völker, D., Geersen, J., Contreras-Reyes, E. and Reichert, C., 2013. Sedimentary fill of the Chile Trench (32°–46°S): volumetric distribution and causal factors. *J. Geol. Soc. London*, **170**, 723–736. doi:doi.org/10.1144/jgs2012-119.

Received 12 November 2015; revised version accepted 7 April 2016

Supporting Information

Additional Supporting Information may be found in the online version of this article:

Figure S1. The Reloca Slide is an exceptionally evident product of a mass-wasting event because of the proximity of the evacuation area and the displaced material and also because of the good preservation and the textbook morphology of both.

Figure S2. Geersen et al. (2011) reported three Pleistocene giant slope failures in the Arauco area in central Chile (36.5°–39°S): Isla Santa María Slide (~388 km^3), Arauco Slide (~253 km^3) and the Mocha Slide (~472 km^3).

Figure S3. Coseismic slip model of the Maule megathrust earthquake Mw 8.8 (February 27, 2010).

Figure S4. (A) Location of seismic stations (orange dots and red triangles) of which data examples are shown in Fig. S5. (B) Velocity–depth model shown in Fig. 4A.

Figure S5. Examples of wide-angle seismic data with predicted travel times (colour curves), which are computed based on the velocity model presented in Fig. 4A. Black bars denote the traveltime picks. (A) OBS 904, (B) OBS 910, and (C) OBS 913.

Figure S6. Derivative Weight Sum (DWS) for rays travelling throughout model shown in Fig. 4A using (A) all rays and (B) rays associated with P-waves recorded only by OBH/OBS's.

Figure S7. (a) Relation between the wedge geometry (α, β) and the direction of principal internal stresses (σ_1, σ_3). (b) Rupture envelope of the non-cohesive critical Coulomb wedge theory in the α-β domain [Figure modified from Maksymowicz (2015)].

Figure S8 (a) Location of the five modelled gravity lines by Maksymowicz et al. (2015). (b and c) Blue numbers correspond to the modelled μ_b in the case of a wedge characterized by hydrostatic internal pressure.